REPORT DOCUMENTATION PAGE

AFRL-SR-AR-TR-04-

0183

1. REPORT DATE (DD-MM-YYYY)	2. REPORT TYPE	3. DATES COVERED (From - To)
04/22/2004	Final	09/01/2001 - 02/14/2003

4. TITLE AND SUBTITLE
PBG Cavity in NV-Diamond for Large Scale Type II Quantum Computing (QC THEMES)

5a. CONTRACT NUMBER

5b. GRANT NUMBER
F49620-01-1-0520

5c. PROGRAM ELEMENT NUMBER

6. AUTHOR(S)
Dr. Selim Shahriar

5d. PROJECT NUMBER

5e. TASK NUMBER

5f. WORK UNIT NUMBER

7. PERFORMING ORGANIZATION NAME(S) AND ADDRESS(ES)

Research Laboratory of Electronics
Massachusetts Institute Of Technology
77 Massachusetts Avenue
Cambridge, MA 02139

8. PERFORMING ORGANIZATION REPORT NUMBER

9. SPONSORING / MONITORING AGENCY NAME(S) AND ADDRESS(ES)
Air Force Office of Scientific Research
4015 Wilson Boulevard
Arlington, VA 22203-1954

20040423 044

12. DISTRIBUTION / AVAILABILITY STATEMENT

Distribution Statement A: unlimited

13. SUPPLEMENTARY NOTES

The objective of this project was to investigating the feasibility of realizing a type II quantum computer (QC) on a large scale, using nitrogen-vacancy color centers in diamond (NV-Diamond). To see the basic mechanism behind this scheme, consider a small volume of this medium. A laser beam incident on this volume can interact with all the centers in this volume. However, each center has a transition frequency that is slightly different from that of the others, a feature known as inhomogeneous broadening. This implies that individual centers can be addressed distinctively by tuning the laser. . In order to perform two qubit operations, such as the controlled-NOT (CNOT), it is necessary to couple two centers that are spectrally adjacent. One mechanism for such a coupling is the dipole-dipole interaction. However, since the spectral neighbors are not necessarily close to each other spatially, it is necessary to enhance this interaction artificially. This can be achieved by embedding the centers in a high-Q optical cavity. A key challenge in realizing this scheme is the cavity. If one were to embed the NV-diamond crystal inside a bulk-mirror based cavity, the residual reflection from the crystal surfaces would degrade the Q to an unacceptable level. A photonic band gap (PBG) cavity holds the best promise to overcome this constraint. The small mode volume of the PBG cavities (on the order of λ_3) implies that the coupling of cavity photons to atoms in the cavity will be enhanced by three or more orders of magnitude over conventional bulk-mirror based cavity couplings. Another key feature of this approach is that the whole substrate will contain many QC's that can be operated simultaneously. Such a structure is ideally suited for type II

15. SUBJECT TERMS

16. SECURITY CLASSIFICATION OF:			17. LIMITATION OF ABSTRACT	18. NUMBER OF PAGES	19a. NAME OF RESPONSIBLE PERSON
a. REPORT	b. ABSTRACT	c. THIS PAGE			19b. TELEPHONE NUMBER (include area code)

PBG Cavity in NV-Diamond for Large Scale Type II Quantum Computing

Grant# : F49620-01-1-0520
OSP#: 6892565

FINAL REPORT

Principal Investigator:
Dr. Selim Shahriar, Principal Research Scientist,
Research Laboratory of Electronics, MIT

ABSTRACT

The objective of this project was to investigating the feasibility of realizing a type II quantum computer (QC) on a large scale, using nitrogen-vacancy color centers in diamond (NV-Diamond). To see the basic mechanism behind this scheme, consider a small volume of this medium. A laser beam incident on this volume can interact with all the centers in this volume. However, each center has a transition frequency that is slightly different from that of the others, a feature known as inhomogeneous broadening. This implies that individual centers can be addressed distinctively by tuning the laser. . In order to perform two qubit operations, such as the controlled-NOT (CNOT), it is necessary to couple two centers that are spectrally adjacent. One mechanism for such a coupling is the dipole-dipole interaction. However, since the spectral neighbors are not necessarily close to each other spatially, it is necessary to enhance this interaction artificially. This can be achieved by embedding the centers in a high-Q optical cavity. A key challenge in realizing this scheme is the cavity. If one were to embed the NV-diamond crystal inside a bulk-mirror based cavity, the residual reflection from the crystal surfaces would degrade the Q to an unacceptable level. A photonic band gap (PBG) cavity holds the best promise to overcome this constraint. The small mode volume of the PBG cavities (on the order of λ^3) implies that the coupling of cavity photons to atoms in the cavity will be enhanced by three or more orders of magnitude over conventional bulk-mirror based cavity couplings. Another key feature of this approach is that the whole substrate will contain many QC's that can be operated simultaneously. Such a structure is ideally suited for type II quantum computing on a large scale. Such a QC may enable efficient computation of complex fluid dynamics, for example. In order to attain this objective, we proposed to use a variation of the method demonstrated by Masuda et al. to realize the PBG structure necessary for quantum computing. First, a custom-mask would be made using lithographic techniques. The pattern on the mask would then be transferred to an NV-diamond crystal surface using chemical etching. The resulting structure would consist of a two dimensional periodic array of holes, with periodicity of the order of the wavelength (λ~637 nm) of interest. The symmetry would be broken by replacing a 3X3 grid of these holes with a hole of a larger diameter. The area around this anomalous hole will constitute the cavity, with a mode volume of the order of a few λ^3. Many such cavities would be formed on the same substrate. Immediately upon the start of this project, the PI accepted a faculty position at the Northwestern University, Evanston, IL. As such, the duration of the effort was reduced to one year, with a no cost extension for one semester. Given the disruption in the personnel availability, as well as the move of the experimental facilities, the effort was limited in its scope, emphasizing (a) modeling of cavity parameters, (b) identification of lithographic steps, and (c) development of algorithms that could benefit from the specific QC model described above.

REPORT DOCUMENTATION

1. LIST OF PUBLICATIONS AND MANUSCRIPTS:

Published in Journals:

1. "Cavity Dark State for Quantum Computing," M.S. Shahriar, J. Bowers, S. Lloyd, P.R. Hemmer, and P.S. Bhatia, *Opt. Commun.* **195**, 5-6 (2001).
2 . "Raman Excited Spin Coherence in NV-Diamond," P.R. Hemmer, A.V. Turukhin, M.S. Shahriar, and J.A. Musser, *Opt. Letts.* **26**, 6 (2001).
4. "Observation of Ultraslow and Stored Light Pulses in a Solid," A. V. Turukhin, V.S. Sudarshanam, M.S. Shahriar, J.A. Musser, B.S. Ham, and P.R. Hemmer, *Phys. Rev. Lett.* **88**, 023602 (2002).
5. "Solid-state Quantum Computing using Spectral Holes," M.S. Shahriar, P.R. Hemmer, P.S. Bhatia, S. Lloyd, and A.E. Craig, *Phys. Rev. A.*, **66**, 032301 (2002)

Conference Presentations:
1. "Raman Excited Spin Coherence in NV Diamond," P.R. Hemmer, A. Turukhin, M.S. Shahriar, and J.A. Musser, *proceedings of the International Quantum Electronics Conference*, Baltimore, MD, 2001.
2. "Observation of Ultraslow Group Velocity of Light in a Pr:YSO crystal," V.S. Sudarshanam, M.S. Shahriar, and P.R. Hemmer, *31st Winter Colloquium in Quantum Electronics*, Snowbird, Utah, 2001.
3. "First Observation of Ultraslow Group Velocity of Light in a Solid," A. Turukhin, V.S. Sudarshanam, M.S. Shahriar, J.A. Musser, and P.R. Hemmer, proceedings of the *International Quantum Electronics Conference*, Baltimore, MD, 2001.
4. "Spin Mediated Slowing and Stoppage of Light in a Solid," A.V. Turukhin, M.S. Shahriar, J.A. Musser, and P.R. Hemmer, *proceedings of Spintech 1*, Maui, Hawaii, 2001.
5. "First Observation of Ultraslow Group Velocity of Light in a Solid," A. Turukhin, V.S. Sudarshanam, M.S. Shahriar, J.A. Musser, and P.R. Hemmer, *proceedings of the SPIE Conference,* San Diego, CA 2001.
6. "Raman Excited Spin Coherence in NV Diamond," P.R. Hemmer, A. Turukhin, M.S. Shahriar, and J.A. Musser, *proceedings of the SPIE Conference,* San Diego, CA 2001 **(Invited)**.
7. "Quantum Computing using NV-Diamond," M.S. Shahriar, presented at *the Progress in Quantum Electronics conference*, Snowbird, UT, Jan. 2002 **(Invited)**.

2. REPORT OF INVENTIONS

- *Demonstrated technique for near-perfect spin alignment in NV-diamond for applications to quantum computing*
- *Developed photonic band-gap cavity design in NV-Diamond for coupling quantum bits*
- *Developed a method for creating entanglement between two qubits using transfer of quantum coherence via non-degenerate sub-levels, a process essential for realizing a quantum computer in NV-diamond*
- *Developed a method for realizing controlled-NOT gates in NV-diamond via direct dipole-dipole coupling between qubits that are spatially adjacent, and can be tuned to become spectrally adjacent using time-dependent magnetic fields.*
- *Developed a method for coupling quantum bits robustly using cavity dark states*
- *Developed a detailed model for quantum computing using NV-diamond*

3. SCIENTIFIC PROGRESS AND ACCOMPLISHMENTS

The objective of this project was to investigating the feasibility of realizing a type II quantum computer (QC) on a large scale, using nitrogen-vacancy color centers in diamond (NV-Diamond). To see the basic mechanism behind this scheme, consider a small volume of this medium. A laser beam incident on this volume can interact with all the centers in this volume. However, each center has a transition frequency that is slightly different from that of the others, a feature known as inhomogeneous broadening. This implies that individual centers can be addressed distinctively by tuning the laser. . In order to perform two qubit operations, such as the controlled-NOT (CNOT), it is necessary to couple two centers that are spectrally adjacent. One mechanism for such a coupling is the dipole-dipole interaction. However, since the spectral neighbors are not necessarily close to each other spatially, it is necessary to enhance this interaction artificially. This can be achieved by embedding the centers in a high-Q optical cavity. A key challenge in realizing this scheme is the cavity. If one were to embed the NV-diamond crystal inside a bulk-mirror based cavity, the residual reflection from the crystal surfaces would degrade the Q to an unacceptable level. A photonic band gap (PBG) cavity holds the best promise to overcome this constraint. The small mode volume of the PBG cavities (on the order of λ^3) implies that the coupling of cavity photons to atoms in the cavity will be enhanced by three or more orders of magnitude over conventional bulk-mirror based cavity couplings. Another key feature of this approach is that the whole substrate will contain many QC's that can be operated simultaneously. Such a structure is ideally suited for type II quantum computing on a large scale. Such a QC may enable efficient computation of complex fluid dynamics, for example. In order to attain this objective, we proposed to use a variation of the method demonstrated by Masuda et al. to realize the PBG structure necessary for quantum computing. First, a custom-mask would be made using lithographic techniques. The pattern on the mask would then be transferred to an NV-diamond crystal surface using chemical etching. The resulting structure would consist of a two dimensional periodic array of holes, with periodicity of the order of the wavelength (λ~637 nm) of interest. The symmetry would be broken by replacing a 3X3 grid of these holes with a hole of a larger diameter. The area around this anomalous hole will constitute the cavity, with a mode volume of the order of a few λ^3. Many such cavities would be formed on the same substrate. Immediately upon the start of this project, the PI accepted a faculty position at the Northwestern University, Evanston, IL. As such, the duration of the effort was reduced to one year, with a no cost extension for one semester. Given the disruption in the personnel availability, as well as the move of the experimental facilities, the effort was limited in its scope, emphasizing (a) modeling of cavity parameters, (b) identification of lithographic steps, and (c) development of algorithms that could benefit from the specific QC model described above.

3.1 Cavity Dark States For Robust Coupling Of Quantum Bits

In recent years, there have been a wide range of activities aimed at quantum computing. A quantum computer with a large number of bits may help solve certain

problems much more efficiently than its classical counterpart[1-3]. While the theoretical work[4-13] has progressed rapidly, the experimental realization [14-17] of a many bit quantum computer remains to be a daunting challenge[14-17]. It is not clear, for example, whether NMR or trapped-ion based quantum computing can be scaled to a large number of qubits. As such, novel approaches are being proposed and pursued by many groups. Some of these proposals involve a collection of distinct quantum systems (such as atoms, molecules, or quantum dots) that are not directly coupled to one another. Instead, an effective coupling is induced via interaction of these quantum systems to an optical cavity.

Pellizari et al. proposed a scheme where each atom has a pair of identical Λ-system transitions[7]. To summarize this scheme briefly, consider the case where two spatially separated but spectrally identical atoms are coupled using a cavity. This is illustrated in Figure 1, where we have shown only one of the two Λ transitions in each atom. Here, one leg of the Λ transition in each atom is simultaneously excited by the photons of the cavity mode, while the remaining legs are excited by classical laser beams, applied externally, as shown in fig. 1a. In the limit where the cavity mode has only zero or one photon, the atoms-field coupled states are shown in fig. 1b. This system has a non-trivial dark state, which can be written as a superposition of the three states that do not contain any component of the atomic excited state, as well as a trivial dark state (shown uncoupled at the bottom of the figure). Such a system can be used to transfer quantum information between the two atoms, using adiabatic following, and also to perform quantum logic when each atom has a pair of identical Λ transitions[7,18-20].

During the transfer, the system evolves adiabatically, while in a superposition of these dark states. As such, this process is impervious to any decoherence caused by spontaneous emission from atomic excited states. However, the non-trivial dark state contains a component corresponding to one photon in the cavity. As such, any cavity decay causes the system to decohere. Since the cavity lifetime is often at least as short as the atomic excited state lifetime, the potential benefit of using the dark state is mitigated substantially. Furthermore, there are situations where the cavity decay rate is orders of magnitude bigger than the linewidth of the atomic system, so that the benefit of using the dark state is minimal. For example, we have recently proposed a scheme where this approach can be used to couple spectrally distinct atoms in a spectral hole burning crystal for quantum computing[21,22]. One candidate system for implementing such a scheme is a cryogenically cooled, thin layer of Pr:YSO, embedded in a cavity. In this case, the atomic excited state is very longed lived (160 μsec), compared to typical cavity lifetimes (10's of nano seconds).[17,23] As such, avoiding the atomic excited state at the cost of populating the photon mode is counter productive.

We have developed a solution to this problem, by using a scheme where the information exchange takes place through a *dark state of the cavity*, which contains no cavity photons, while a finite population of the atomic excited state is allowed for a short time. To see how such a state might be formed, consider the level diagram of figure 2.[24] The objective here is to find a dark state that does not contain the middle state (with 1 photon in the cavity), and contains as small a fraction as possible of the states with components of the atomic excited state. By detuning the classical fields, while keeping the cavity resonant, we find that we can produce a state which has no photons in the cavity mode: a cavity dark state. This state does not contain any significant component

of $|b_1b_21\rangle$, and has a small component (proportional to $|\Omega/\delta|^2<<1$) of states containing the atomic excited states. This state is produced by combining the strong-field seeking dressed states corresponding to the two-level transition in each atom, in the limit where $|\Omega/\delta|^2<<1$. Explicitly, the cavity-dark-state is given by:

$$|DC\rangle \propto \Omega_2\left(|a_1b_20\rangle + \frac{\Omega_1}{2\delta}|c_1b_20\rangle\right) - \Omega_1\left(|b_1a_20\rangle + \frac{\Omega_2}{2\delta}|b_1c_20\rangle\right)$$

Since this state does not contain any photons, it is impervious to the cavity decay, in the same manner that a conventional dark state is unaffected by atomic decay. Of course, this state is not completely dark with respect to the atomic decay. However, the effect of atomic decay is reduced by a factor of $|\Omega/\delta|^2$, which can be made small by increasing the detuning. Moreover, since the atomic decay rate in Pr:YSO is much smaller than the decay rate of the cavity, this state is particularly suited for our scheme.

The potential success of this model depends strongly on the details of the adiabatic following. It is necessary to determine the conditions under which the system can be made to evolve in this state during the counter intuitive pulse sequence used for the transfer. We have looked at this issue in detail, and have identified conditions under which the transfer takes place in a state that is very close to this cavity dark state.

In general, during the adiabatic passage, the system is susceptible to decoherence from several sources. To minimize decoherence effects, it is desirable to complete the adiabatic passage as quickly as possible. But, as the passage time becomes shorter, nonadiabatic effects are introduced. While nonadiabaticity is not a decoherence effect, it can of course cause the coherent transfer to fail, and it can cause the system to become more susceptible to decay as a result of populating unstable states. To use adiabatic passage for coherent transfer, the actual passage time must be carefully optimized: fast enough to be adiabatic, but slow enough to avoid significant decay.

The defining parameters of the system are the vacuum Rabi frequency g, the cavity decay rate κ, and the spontaneous emission rate γ. The vacuum Rabi frequency g is determined by the cavity geometry and the strength of the atomic dipole moment; κ depends on the cavity geometry, the reflectivity of the cavity mirrors, and the presence of scattering centers within the cavity; γ is determined from the atomic dipole moment (we will assume that the decay rate inside the cavity does not differ significantly from the free space rate). Here, we assume that these parameters are fixed, and determine how a variation of the control parameters can be used to improve the quality of adiabatic passage.

For notational simplicity, we rename the five basis states of figure 3 as follows: $|1\rangle=|ab0\rangle$, $|2\rangle=|cb0\rangle$, $|3\rangle=|bb1\rangle$, $|4\rangle=|bc0\rangle$, $|5\rangle=|ba0\rangle$, as shown. Consider a situation where the system is in the state $|1\rangle$ at t=0. The counter-intuitive pulse sequence is applied as follows: Ω_1 is kept zero and Ω_2 is turned on for a duration T_1. At $t=T_1$, Ω_1 is also turned on over a duration T while Ω_2 is turned off. At $t=T_1+T$, Ω_1 is also turned off over a duration T_2, and the operation is complete at $t=T_1+T+T_2$. . Obviously, the transfer has to take place during the time when both fields are non-zero, i.e., during the interval T. Figure 3a shows the energies of the five eigenstates of the system during this interval. Here, the unit of energy is chosen to be $\hbar g=1$, the peak value of Ω_1 and Ω_2 is $\Omega_o=10g$,

and the detuning is δ=-100g. Note that the states |2>, |3> and |4> are degenerate (in the rotating wave frame) in the absence of interactions. We have chosen this to be the zero of energy in this plot. As the laser beams are turned on, these three states evolve into a band of three dressed states, which are shown on an expanded scale in figure 3b. Similarly, the states |1> and |5> are degenerate in the absence of interactions, with a energy equaling δ. As the laser beams are turned on, these two states evolve into another band of two dressed states, which are shown on an expanded scale in figure 3c.

It is difficult to express the eigenvectors corresponding to these levels in exact analytic form. However, one can easily derive the approximate form of these states by using well-known expressions for two-level dressed states.[25] Furthermore, this approach allows us to derive approximate analytic expressions for the energy levels as well. In the case considered here, the system starts out in the state denoted by |α> (the solid line in fig 3c). What we need to determine are the conditions under which the system will stay in this state. The state that it can couple to via non-adibaticity is the one denoted by |β> (the dotted line in fig 3c), since it appears to become degenerate with the desired state at the middle of the interaction time.

To interpret the eigenstates and the eigenenergies, consider first the state |5> interacting with state |4>. Assuming that the detuning is much greater than the Rabi frequency, we get the light shifted state:

$$|5'\rangle = |5\rangle + \frac{\Omega_2}{2\delta}|4\rangle$$

where the normalization is omitted since it is approximately unity. At $t \leq T_1$, we thus have $|\alpha\rangle = |1\rangle$ and $|\beta\rangle = |5'\rangle$ with an energy difference given by:

$$\varepsilon \equiv \langle \alpha | H | \alpha \rangle - \langle \beta | H | \beta \rangle = -\frac{\Omega_2^2}{4\delta}.$$

As Ω_1 is turned on, the state |1> is also light shifted, via its interaction with state |2>, producing the state:

$$|1'\rangle = |1\rangle + \frac{\Omega_1}{2\delta}|2\rangle.$$

However, the states |1'> and |5'> are not fully decoupled from each other. We proceed in steps to determine the eigenstates |α> and |β> when both laser fields are nonzero.

Consider the coupling of the light shifted state |1'> to the intermediate state |3>, mediated by the vacuum Rabi frequency, g. The coupling rate is:

$$g_1 = 2\langle 1'| H | 3\rangle = \frac{\Omega_1}{2\delta} \cdot 2 \cdot \langle 2 | H | 3\rangle = \frac{\Omega_1 g}{2\delta}$$

with a detuning (i.e., the energy difference between |1'> and |3>, under the rotating wave transformation) given approximately by δ. Since this detuning is much larger than the coupling strength g_1 the state |1'> is further light-shifted by this interaction, producing the state:

$$|1''\rangle = |1'\rangle + \frac{g_1}{2\delta}|3\rangle.$$

Similarly, the state |5'> interacts with state |3> to produce the light-shifted state:

$$|5''\rangle = |5'\rangle + \frac{g_2}{2\delta}|3\rangle$$

where $g_2=2\langle 5'|H|3\rangle=\Omega_2 g/2\delta$. The energy difference between |1''> and |5''> is now given by:

$$\Delta = \left(\Omega_2^2 - \Omega_1^2\right)\cdot\left(\frac{1}{4\delta} + \frac{g^2}{16\delta^3}\right) \approx \left(\Omega_2^2 - \Omega_1^2\right)/4\delta .$$

The states |1''> and |5''> couple to each other as well, since each contains a component of state |3>. The coupling rate is:

$$G = 2\langle 1''|H|5''\rangle = \frac{g_1^2}{2\delta} + \frac{g_2^2}{2\delta} = \frac{g^2}{8\delta^3}\cdot 2\Omega_1\Omega_2 .$$

Diagonalizing this interaction G in the presence of the detuning Δ yields the eigenstates:

$$|\alpha\rangle = \cos\theta\cdot|1''\rangle - \sin\theta\cdot|5''\rangle$$

$$|\beta\rangle = \sin\theta\cdot|1''\rangle + \cos\theta\cdot|5''\rangle$$

where $\tan 2\theta = G/\Delta$, and the energy separation is given by $\varepsilon = \sqrt{\Delta^2 + G^2}$.

Before proceeding further, it instructive to consider this result in the limits. Just at the onset of the active period T, we have $\Omega_1=0$, so that G=0 and $\Delta=\Omega_2^2/4\delta$, yielding $\varepsilon=\Omega_2^2/4\delta$, as determined before. Since θ=0, the eigenstates are given by |α>=|1''>=|1'>=|1> and |β>=|5''>=|5'>, again as determined before. At the end of the period T, we have have $\Omega_2=0$, so that G=0 and $\Delta=\Omega_1^2/4\delta$, yielding $\varepsilon=\Omega_1^2/4\delta$, as expected. Now θ=π/2 and the eigenstates are given by -|α> =|5''>=|5'>=|5> and |β>=|1''>=|1'>=|1>, as wanted. Finally, at the cross-over point, $\Omega_1=\Omega_2=\Omega_o/\sqrt{2}$, so that Δ=0 and $G=g^2\Omega_o^2/8\delta^3$, yielding $\varepsilon= g^2\Omega_o^2/8\delta^3$, in close agreement with the energy separation shown in figure 4, which is an expanded view of the anti-crossing region of figure 3c. Here θ=π/4 and the eigenstates are:

$$|\alpha\rangle = \frac{1}{\sqrt{2}}\left(|1''\rangle - |5''\rangle\right) = \frac{1}{\sqrt{2}}\left(|1'\rangle - |5'\rangle\right)$$

$$|\beta\rangle = \frac{1}{\sqrt{2}}\left(|1''\rangle + |5''\rangle\right) = \frac{1}{\sqrt{2}}\left(|1'\rangle + |5'\rangle + \frac{g\Omega_o}{2\delta^2}|3\rangle\right)$$

Thus, the state |α> is exactly dark with respect to the cavity mode at this point.

During adiabatic following, the system parameters must change slowly compared to the energy separation between these two eigenstates. More quantitatively, we can say that the rate of mixing between these two states, Q_{NA}, must be constrained by:

$$Q_{NA} \equiv \left\langle \alpha \left| \frac{\partial}{\partial t} \right| \beta \right\rangle \le \frac{\varepsilon}{\xi}$$

where ξ is the adiabaticity parameter. Typically, a value of ξ=10 or greater ensures that the system will stay primarily in the state |α> during the evolution. For example, in the case where ε is kept constant during the evolution, the adiabaticity constraint can be interpreted simply as the transit time broadening of the energy levels due to the finite time of interaction. The inverse of the transit time (which is characteristic of the rate of mixing between the dressed states) then must be less than the energy separation ε by the

factor of ξ in order to assure that the levels do not get too close to each other. In the case at hand, however, ε varies with time. In order to minimize the time necessary for the adiabatic transfer, we adopt the method where the rate of change of the two Rabi frequencies are varied dynamically as the value of ε changes.

In order to constrain time variations of the two Rabi frequencies (for computational simplicity), we consider an equivalent model where the two laser beam profiles are fixed in time, and vary in space sinusoidally (or cosinusoidally), extending over a distance L: $\Omega_1(x)=\Omega_0 Sin(x\pi/2L)$, $\Omega_2(x)=\Omega_0 Cos(x\pi/2L)$. The atom plus cavity is then assumed to travel through the field profile, at a speed $v(t)$ that varies with time. Once the exact functional form of this time varying speed is determined, the total travel time T is found by inverting the relation:

$$L = \int_0^T dt \cdot v(t).$$

In order to determine $v(t)$, we estimate first the non-adiabatic coupling rate, Q_{NA}, using the explicit expressions for the eigenstates determined above. The resulting expression is quite cumbersome. In order to simplify further, we note first that:

$$\tan(2\theta) = \frac{G}{\Delta} = \eta \tan(\pi x / L); \qquad \eta \equiv \frac{g^2}{2\delta^2}.$$

Given that η is very small, we can identify two distinct zones during the adiabatic transfer. For a very small zone $L/2-d/10<x<L/2+d/10$ (where $d=\eta L/\pi$) around the center ($x=L/2$), we have $G>>\Delta\approx 0$, so that $\theta\approx\pi/4$ and $\varepsilon\approx G$. Once we get away from the center by a distance of more than $\pm 10d$ we have $\Delta>>G$, so that $\varepsilon\approx\Delta$, $\mathrm{Cos}(\theta)\approx 1$, and $\mathrm{Sin}(\theta)\approx\theta\approx G/2\Delta$. The velocity in the intermediate zone can be estimated via interpolation. The resulting total time for adiabatic transfer is given by $T\approx \xi/9\varepsilon_{min}$, where ε_{min} is the minimum separation between the energies of the eigenstates, given by $g^2\Omega_o^2/4\delta^3$, as determined before. For $\xi=10$, we have verified via numerical methods that this value of T results in nearly perfect adiabatic transfer.

As an explicit example, consider the case where $\Omega_0=g=\delta/3$, so that all our approximations remain valid. We then have $\varepsilon_{min}\approx 10^{-2}g$, and the time for adiabtic transfer is $T\approx 12\xi g^{-1}$. This is about an order of magnitude slower than the time needed for the Pellizari scheme. However, the effect of cavity decay, integrated over the transfer time, is now much smaller. Explicitly, the maximum population of the state $|3>$ is about $0.4\mathrm{X}10^{-4}$, as compared to 1/3 for the Pellizari case. The effective rate of decoherence due to cavity photon decay is thus reduced by nearly three orders of magnitude. Thus, the cavity dark state described here achieves the desired transfer of quantum information without being affected significantly by the cavity decay, and yet does not take much longer than the original Pellizari scheme.

To summarize, we have shown that two multilevel atoms can perform quantum communication with each other via interaction with an enclosing cavity containing virtually no photons at all times. The physical mechanism is analogous to the way populations can be exchanged between the extremal states in a three level system via adiabatic following, without populating the intermediate states. The combined system of the two atoms, the cavity, and two laser beams contains a dark state corresponding to the

cavity in its ground state. Using a counter-intuitive pulse sequence, quantum information can be transferred adiabatically from one atom to the other via this cavity dark state. This process can be used to circumvent the effect of cavity decay in a quantum computer formed by interconnected qubits. Finally, it should be possible to generalize this model to other situations where a damped channel is used to couple stable systems.

References:

1. Shor, Peter W. LANL quant-ph archive, preprint 9508027, 1996.
2. Grover, Lov K., *Phys.Rev. Lett* **79**, 325 (1997).
3. A. Ekert and R. Jozsa, *Rev. Mod. Phys.* **68**, 733 (1996).
4. S. Lloyd, *Science*, **261**, 1569 (1993).
5. D.P. DiVincenzo, *Science*, **270**, 255 (1995).
6. J.I. Cirac and P. Zoller, *Physical Review Letters*, **74**, 4091 (1995).
7. Pellizzari, T., Gardiner, S.A., Cirac, J.I., Zoller, P. *Phys. Rev. Lett.* **75**, 3788 (1995)
8. S. Lloyd, *Physical Review Letters*, **75**, 346 (1995).
9. L. Viola and S. Lloyd, *Physical Review A,* **58**, 2733 (1993)
10. B.E. Kane, *Nature*, **393**, 133 (1998)
11. D. Deutsch, A. Barenco, A. Ekert, *Proceedings of the Royal Society of London A*, **449**, 669 (1995).
12. C.H. Bennett, D.P. DiVincenzo, J.A. Smolin, *Physical Review Letters*, **78**, (1997)
13. S.J. van Enk, J.I. Cirac, and P.Zoller, *Physical Review Letters*, **79**, 5178 (1997)
14. C. Monroe, D.M. Meekhof, B.E. King, W.M. Itano, D.J. Wineland, *Physical Review Letters*, **75**, 4714 (1995)
15. D.G. Cory, A.F. Fahmy, T.F. Havel, *PhysComp96*, Proceedings of the Fourth Workshop on Physics and Computation, T. Toffoli, M. Biafore, J. Leao, eds., New England Complex Systems Institute, 1996, pp. 87-91.
16. N.A. Gershenfeld and I.L. Chuang, *Science*, **275**, 350 (1997).
17. C. J. Hood, M. S. Chapman, T. W. Lynn, and H. J. Kimble, *Physical Review Letters*, **80**, 4157 (1998).
18. J. Kuklinski, U. Gaubatz, F. Hioe, K.Bergmann, *Phys. Rev. A* **40**, 6741 (1989).
19. P.Marte, P.Zoller, J.Hall, *Phys. Rev. A* **44**, R4118 (1991).
20. A. Parkins, P. Marte, P., Zoller, H. Kimble, *Phys. Rev. Lett.* **71**, 3095 (1993).
21. M.S. Shahriar, J. Bowers, S. Lloyd, P.R. Hemmer, and A.E. Craig "Quantum Computing via Cavity-coupled Bands in a Spectral Hole-Burning Solid," Proceedings of the OSA Annual Meeting 1998, Baltimore, MD.
22. B.S. Ham, M.S. Shahriar, and P.R. Hemmer, *Opt. Lett.* **22**, 1138 (1997). B.S. Ham, M.S. Shahriar, M.K. Kim, P.R. Hemmer, *Optics Letters, Vol.* **22**, 1849 (1997).
23. R.W. Equall, R.L. Cone, and R.M. Macfarlane, *Physical Review B*, Vol. **52**, 3963-69 (1995).
24. For simplicity, we have used the original model of ref. 7 where the two atoms are spectrally identical; it can be generalized easily to the scheme for coupling spectrally adjacent atoms.
25. M.S.Shahriar, P.R.Hemmer, D.P.Katz, A. Lee, and M.G. Prentiss, *Phys. Rev. A* **55**, 2272 (1997).

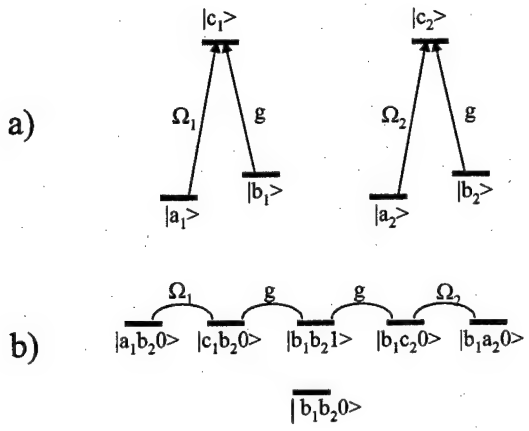

Figure 1. a) Illustration of the coupling of two atoms using the dark resonance inside a cavity Here, g is the vacuum Rabi frequency of the cavity, $\Omega_1(\Omega_2)$ is the Rabi frequency of the first(second) laser beam. b) The atom cavity composite states (rotating wave frame) corresponding to two of the closed transition manifolds having a maximum of 1 or 0 cavity photons. The ket notation for the composite states is indexed by the internal states of the first and second atoms followed by the photon number in the cavity mode.

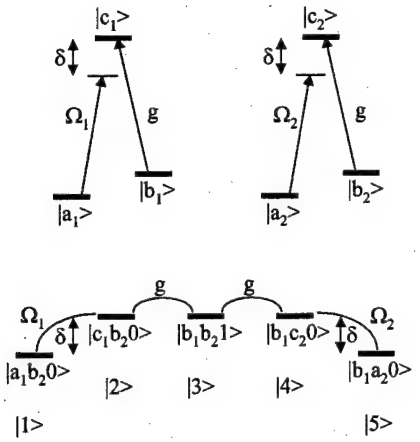

Figure 2. Illustration of the excitation scheme needed to implement a cavity dark state. As shown in the top diagram, the classical laser beams are detuned, while the cavity is kept on resonance. The bottom diagram shows the same situation in the rotating wave frame. The state $|b_1 b_2 0\rangle$ (not shown) is still the trivial dark state.

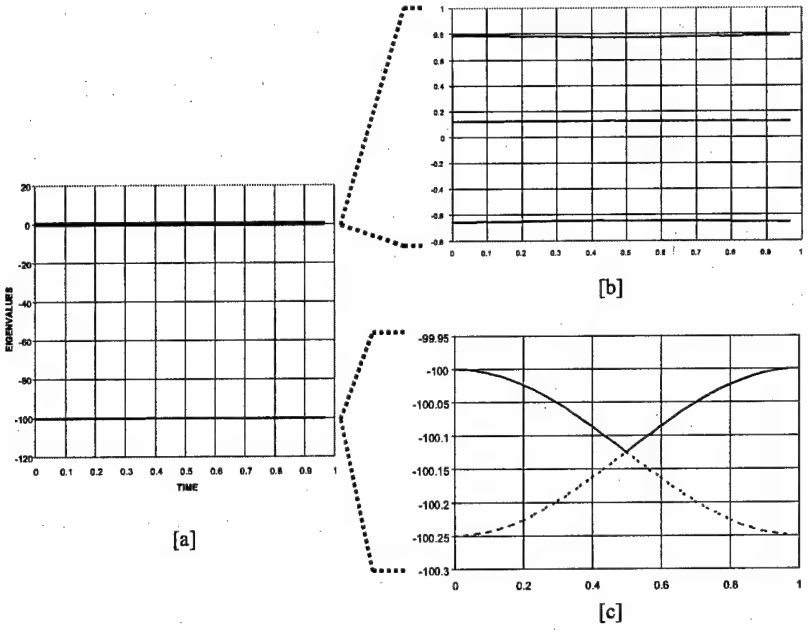

Figure 3. Illustration of the dressed states corresponding to the system of two atoms coupled to the cavity, as functions of the interaction interval during which both laser pulses are present. (a) All five dressed states on the same scale (b) Expanded view of the dressed states that evolve adiabatically from/to the states |2>, |3> and |4> (c) Expanded view of the dressed states that evolve adiabatically from/to the states |1> and |5>.

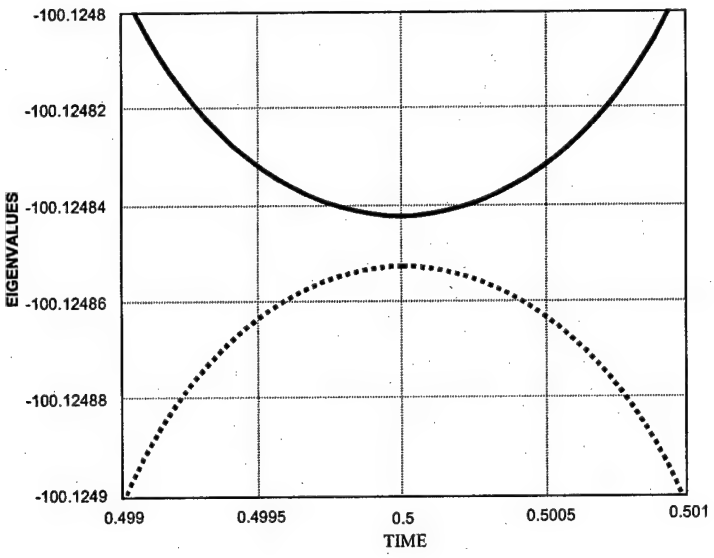

Figure 4. Expanded view of the anti-crossing of the dressed states at the center. The separation at the center is about $1.2x10^{-5}$, in close agreement with the analytical result of $1.25x10^{-5}$, both expressed in units of $\hbar g$.

3.2 Controlled-NOT using Direct Dipole-Dipole coupling in NV-Diamond:

If the effective density of color centers is high, then one can make use of the direct dipole-dipole coupling between color centers. The basic dipole-dipole coupling scheme has been developed by affiliate members of our project. Briefly, two atoms (or color centers) must be identified that are spatially separated by a distance of less than $\lambda/10$ where λ is the optical wavelength of a convenient Raman transition. The optical transitions of the two atoms must also be close enough that components of the Raman transitions on neighboring atoms can be tuned to the same wavelength on demand using for example magnetic fields.

For illustrative purposes, consider an existing sample of diamond with N-V color centers with dipole allowed zero-phonon optical transition at 637 nm. The N-V center concentration of this diamond (on loan to us) is ~30 ppm, which corresponds to 5×10^{18} centers/cc. To achieve a high-fidelity CNOT using dipole interactions, a spatial separation of less than $\lambda/12$ between centers is assumed, since this gives an optical line splitting of 10 times its homogeneous linewidth (of 50 MHz). In a volume of $(\lambda/12)^3$ there are about 900 centers. Based on the 750 GHz inhomogeneous width, this gives an average spectral separation of 1.2 GHz (Fig. 1). Using Zeeman shifts, this frequency offset can be spanned with a variable magnetic field, tuned over a 0.6 kG range. In this example, operations would be performed on the time scale of nanoseconds. Given the spin lifetime of 0.1 msec in N-V diamond, this translates to 1000s of operations per spin lifetime.

The experiments can proceed in several stages of increasing difficulty, using previously demonstrated techniques wherever possible. In the first stage, individual N-V color centers can be observed at room temperature in a lightly doped sample, as previously demonstrated elsewhere. This can be accomplished two ways. First, the sample can be flood-illuminated with an argon laser beam at 514 nm. After passing through a holographic notch filter, the fluorescence can be imaged onto a single-photon grade image intensifier. The output of the intensifier can in turn be imaged onto an integrating CCD camera (ICCD)(see Fig. 2a.) To detect images at the single photon level, the output of the camera can be input to a real-time frame accumulator and image processor card. This imaging system can be used to identify interesting regions of the sample and for day-to-day repeatability by insuring that the same sample location is probed each time.

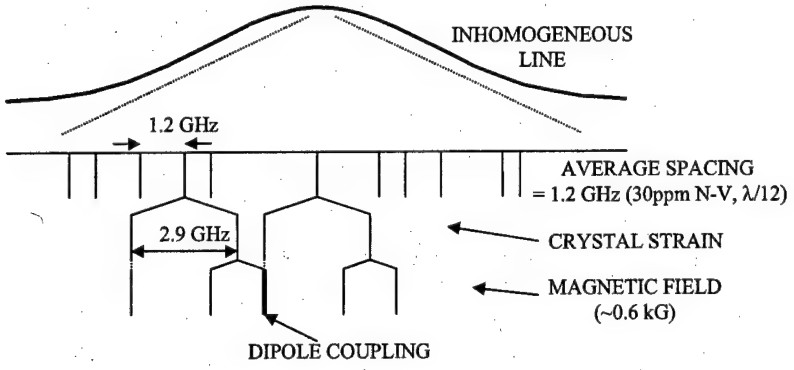

Figure 1. Illustration of spectral density of N-V color centers in diamond in a volume of $(\lambda/12)^3$ with 30 ppm concentration.

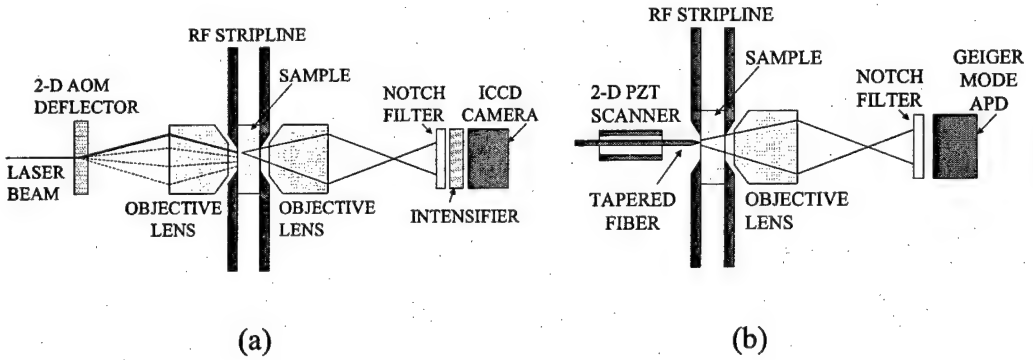

Figure 2. (a) Diagram of experimental setup for probing individual color centers in a diamond sample of moderate doping concentration. Initially the scanning laser beam will be replaced by flood-illumination. The integrating video camera (ICCD) will be followed by a frame accumulator. (b) Experimental setup of near-field excitation of coupled dipoles. To perform logic operations better, the video camera will eventually be replaced by a higher quantum efficiency avalanche photodetector (APD).

Next, the flood-illumination can be replaced by a focused argon laser spot that is steered using a 2-D acousto-optic angle scanner (AOM), where the angle is converted into position by a microscope objective lens. This scanner is capable of slow raster scans to verify the local spatial distribution of color centers, but can primarily be configured to steer to a particular angle, so as to illuminate a single color center. Fluorescent light from this color center can then be collected and imaged onto the photon-counting camera system. Once this system has been tested at room temperature, the experiment can be repeated at liquid helium temperature by inserting the sample, with objective lenses, into a cryostat.

After the first low temperature test is complete, the diamond sample can be replaced by one with a higher N-V concentration such that there will be 100-1000 color centers within a focused laser spot. In this case the color centers can only be resolved by using both spatial and spectral techniques and the argon laser illumination will be

replaced by a dye laser tuned within the zero phonon line. As before, a holographic notch filter can be used to reject scattered laser light and detection will be accomplished using phonon sideband fluorescence. Alternatively, backscattered fluorescence can be used for detection, wherein the laser-focusing objective also collects the florescence, which is then diverted by a beamsplitter onto the photon-counting camera system using auxiliary imaging optics.

Within a laser beam focal volume on the order of λ^3, most atoms with similar spectral response will be too far apart to experience large dipole-dipole interactions. However, one in 100 should have interactions large enough to split an optical absorption line by more than its width. This ratio can be improved by finding atoms whose fluorescence intensity falls off at the same rate when the focused laser spot is moved slightly in the x or y directions. The image subtraction capability available in the image accumulator/processing system can facilitate this. Once a suitable pair of color centers has been identified, a CNOT experiment can then be performed, noting that diamond N-V color centers are exceptionally stable and are expected to remain unchanged in properties, even with repeated laser excitation. Initially, a quasi cw experiment can be performed wherein it is verified that the splitting of an absorption line can be turned on or off by changing only the ground state which the control atom occupies. This will demonstrate that a CNOT is possible. Next a pulsed version of a CNOT can be implemented. It is anticipated that this pulsed experiment will require higher fluorescence detection efficiency. At this point, the single-photon imaging system can be replaced by a single-photon counter, based on an avalanche photodiode (APD). The APD has more than an order of magnitude greater photon efficiency at wavelengths above 630 nm. (see Fig. 2b).

To couple more than one pair of color centers, a higher N-V center concentration is needed. In this case, there will be more color centers within a focused laser spot than it will be possible to resolve spectrally. The laser focusing lens will have to be replaced by a near field imaging system consisting of a tapered fiber optic tip with a tip diameter on the order of $\lambda/10$. Typically these tips are made by pulling a length of silica fiber on a modified commercial pipette puller. As shown in Fig. 2b, the x-y-z position of this tip can be controlled by a piezoelectric transducer (PZT), having a cylindrical shape and a 4-segment electrode. In this case fluorescence detection must be accomplished with an objective lens on the opposite side of the sample.

The goal of these experiments is to use previously demonstrated techniques to perform single color center spectroscopy of N-V diamond in the near dipole-dipole coupling regime. Once this has been achieved, the feasibility of a CNOT can be demonstrated spectroscopically by adjusting initial ground state populations and applying the appropriate pulses.

3.3 FDTD Based Design of a Photonic Band Gap Cavity in an NV-Diamond Substrate

One of the most important criteria in making a quantum computer is that one must be able to realize a CNOT operation between two nearest-neighbor qubits. We have

identified in explicit detail two different methods for achieving this objective in NV-diamond. The first method, applicable to high-density of color centers, uses the direct optical dipole-dipole coupling between two qubits that are very close to each other spatially, and can be turned into spectral neighbors via applying a magnetic field. This method is somewhat limited in the number of bits that can be coupled. The second method, applicable to low-density of color centers, uses a high-finesse optical cavity, resonant with a transition common to both bits, to enhance the optical dipole-dipole coupling. The number of qubits that can be realized this way can in principle be as high as 10^5. While such a high number would be difficult to realize in practice, it should be possible to realize a more modest number (~300) qubits without much trouble.

For efficient cavity-induced coupling, a high value of Q ($2X10^5$) is achievable using the so-called super-mirrors, manufactured by the Research Electro Optics, Inc., of Boulder, CO. However, this number is virtually impossible to achieve in the presence of NV-diamond between the cavity mirrors. Even a small amount of loss resulting, for example, from Fresnel reflections will reduce the Q by orders of magnitude. As such, the idea of using bulk super mirrors of this type is essentially impracticable.

In principle, one could overcome this problem by making the cavity volume small enough so that the ratio of the vacuum rabi-frequency to the cavity decay rate becomes favorable. However, in order to allow unimpeded access of the control-lasers, the separation between the mirror surfaces has to be at least 5 to 10 times the wavelength of interest (λ~637 nm). Furthermore, the machining process used to taper the tips of the mirrors constraints the lateral dimensions to at least a 100 μm. Under these constraints, it is virtually impossible to make the vacuum rabi frequency stronger than the anticipated poor cavity decay rate in the presence of reflection losses from the surfaces of the embedded crystal. A photonic band gap (PBG) cavity holds the best promise to overcome this constraint. The small mode volume of the PBG cavities (on the order of λ^3) implies that the coupling of cavity photons to atoms in the cavity will be enhanced by three or more orders of magnitude over conventional bulk-mirror based cavity couplings. As a result, the number of operations that can be performed before decoherence will be higher by nearly the same ratio.

Another key feature of this approach is that a large number of PBG cavities can be realized on the same substrate. Intercoupled qubits inside each cavity will constitute a single QC. As such, the whole substrate will contain many QC's that can be operated simultaneously. As mentioned above, such a structure is ideally suited for type II quantum computing on a large scale.

We have developed a concrete design to realize a PBG cavity in NV-Diamond in order to demonstrate the feasibility of a QC array where (i) each QC will have a large number of coupled qubits, (ii) the total number of QC's can be very high, as suited for type II quantum computing, and (iii) many operations can be performed before decoherence. We will use a variation of the method demonstrated recently by Masuda et al. to realize the PBG structure necessary for quantum computing. First, a custom-mask will be made using lithographic techniques. The pattern on the mask will then be transferred to an NV-diamond crystal surface using chemical etching. The resulting structure will consist of a two dimensional periodic array of holes, with periodicity of the order of the wavelength (λ~637 nm) of interest. The symmetry will be broken by replacing a 3X3 grid of these holes with a hole of a larger diameter. The area around this

anomalous hole will constitute the cavity, with a mode volume of the order of a few λ^3. Many such cavities will be formed on the same substrate. An important element of our quantum computing protocol requires that the cavity resonance frequency be tunable rapidly, in order to move the coupling process from one set of spectral neighbors to a different one. In order to achieve this capability, the anomalous hole in the center of the cavity will be filled with a non-linear glass. The cavity frequency then can be tuned simply by applying a suitably intense laser beam, which can be done very rapidly.

In order to determine the proper parameters suitable for our model of quantum computing, it is necessary first to simulate this cavity design. There are two established ways of performing these simulations: the Electromagnetic Variational Principle (EVP) method and the Finite Difference Time Domain (FDTD) method. We have developed codes for both methods, and studied the merits and demerits of both methods as pertaining to our specific task here, keeping in mind that we will need to incorporate the Jaynes-Cummings model of quantized fields at some point, in order to consider the coupling between a single photon and a single color center.

The Electromagnetic Variational Principle method:

The starting point for this method is the Maxwell's Equations in the absence of any excess charge or current source:

$$\nabla \cdot \mathbf{B} = 0 \tag{1a}$$

$$\nabla \cdot \mathbf{D} = 0 \tag{1b}$$

$$\nabla \times \mathbf{E} + \frac{1}{c}\frac{\partial \mathbf{B}}{\partial t} = 0 \tag{1c}$$

$$\nabla \times \mathbf{H} - \frac{1}{c}\frac{\partial \mathbf{D}}{\partial t} = 0 \tag{1d}$$

Assuming the fields to be harmonic:

$$\mathbf{H}(\mathbf{r},t)=\mathbf{H}(\mathbf{r})e^{i\omega t} \qquad \mathbf{E}(\mathbf{r},t)=\mathbf{E}(\mathbf{r})e^{i\omega t} \tag{2}$$

we get the following pair of equations:

$$\begin{aligned}\nabla\times\mathbf{E}(\mathbf{r})+\frac{i\omega}{c}\mathbf{H}(\mathbf{r})&=0\\ \nabla\times\mathbf{H}(\mathbf{r})-\frac{i\omega}{c}\varepsilon(\mathbf{r})\mathbf{E}(r)&=0\end{aligned} \tag{3}$$

These equations can be recast in the form:

$$\hat{\Sigma}\,\mathbf{H}(\mathbf{r})=\left(\frac{\omega}{c}\right)^2\mathbf{H}(\mathbf{r}) \tag{4}$$

Where the operator $\hat{\Sigma}$ operating on any vector $\vec{A}$ is defined as:

$$\hat{\Sigma}\,\vec{A}\equiv\nabla\times\left(\frac{1}{\varepsilon(\mathbf{r})}\nabla\times\vec{A}\right) \tag{5}$$

The corresponding electric field is determined by:

$$\mathbf{E}(\mathbf{r})=\left(\frac{-ic}{\omega\varepsilon(\mathbf{r})}\right)\nabla\times\mathbf{H}(\mathbf{r}) \tag{6}$$

Equation (5) can be shown to be formally equivalent to the time-independent Schroedinger Equation (SE) for the wavefunction of a particle in the presence of a potential. As is well-known, the lowest energy eigenstate corresponding to the SE can be determined by using the variational method. Recalling briefly, in this method, one starts with a best-guess wavefunction, and computes the corresponding energy. The parameters of the wavefunction are then varied in the direction that reduces the energy, thus eventually reaching a global minimum as a function of these parameters. The corresponding wavefunction is the lowest energy eigenstate (LEE). This method then can be repeated to find the second lowest energy eigenstate (SLEE), by insisting that the state is orthogonal to the LEE. The process can continue indefinitely to find all the eigenstates of the system. The normal modes of ***H(r)*** as constrained by eqn. 5 can be found by applying the same variational method. The corresponding ***E(r)*** is then given by equation 6.

This method is particularly suited for solving stationery problems, having some degree of symmetry. Specifically, we have investigated a reduced version of our proposed PBG-cavity design using this method, as illustrated in figure 1. Here, the top figure (1a) shows a two dimensional arrangement of dielectric cylinders, with a defect site at the center, represented by a cylinder with a reduced diameter and/or a smaller

index. We assume that the cylinders are of infinite length in the z-direction. A typical field pattern corresponding to this cavity is shown in figure 1b. As can be seen, the mode pattern around the defect site is similar to what was anticipated in the design proposed. However, non-vanishing components of the field elsewhere is also seen to be present. In practice, these non-vanishing components are not likely to affect the basic manner in which the cavity is supposed to be used for coupling qubits.

The next step of the simulation will be to find the field pattern when the cylinders are capped in the z-direction by a pair of confining layers, as outlined in our model. Furthermore, we need to determine the dynamical behavior (such as the lifetime of the mode, which in turn determines the Q). The EVP method is not well suited for this purpose. As such, we have also been exploring the more powerful --- albeit less efficient --- method of FDTD, as described below.

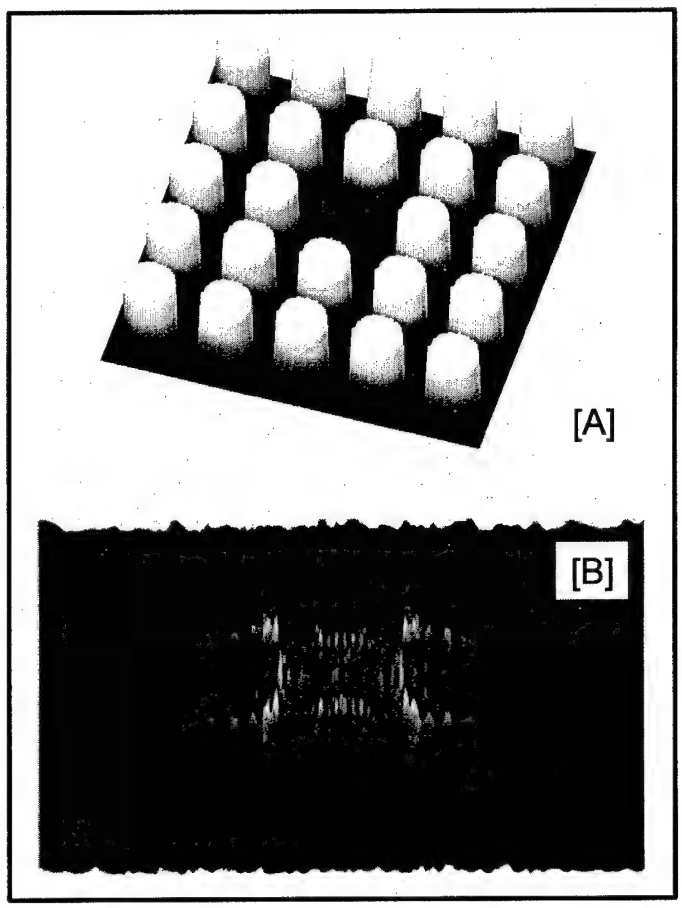

Figure 1: Illustration of the mode pattern in a two-dimensional PBG structure with an embedded defect. Here, the top figure (A) shows a two dimensional arrangement of dielectric cylinders, with a defect site at the center, represented by a cylinder with a reduced diameter and/or a smaller index, or completely absent. We assume that the cylinders are of infinite length in the z-direction. A typical field pattern corresponding to this cavity is shown in the bottom figure (B). As can be seen, the mode pattern around the defect site is similar to what was anticipated in the design proposed in figure 8. However, non-vanishing components of the field elsewhere is also seen to be present. In practice, these non-vanishing components are not likely to affect the basic manner in which the cavity is supposed to be used for coupling qubits.

The Finite Division Time Domain method:

Consider a general, one dimensional scalar wave equation of the form:

$$\frac{\partial^2 u}{\partial t^2} = c^2 \frac{\partial^2 u}{\partial x^2} \tag{7}$$

The function u(x,t) can be expanded about (x+Δx) in a Taylor series of the form:

$$u(x_i + \Delta x, t_n) = u(x_i, t_n) + \Delta x \cdot \frac{\partial u}{\partial x}|_{x_i,t_n} + \frac{\Delta x^2}{2} \cdot \frac{\partial^2 u}{\partial x^2}|_{x_i,t_n} + \frac{\Delta x^3}{6} \cdot \frac{\partial^3 u}{\partial x^3}|_{x_i,t_n} + \frac{\Delta x^4}{24} \cdot \frac{\partial^4 u}{\partial x^4}|_{x_i,t_n} \tag{8}$$

where

$$x_i = i\Delta x, \quad t_n = n\Delta t \tag{9}$$

It can also be expanded about (x-Δx) in the form:

$$u(x_i - \Delta x, t_n) = u(x_i, t_n) - \Delta x \cdot \frac{\partial u}{\partial x}|_{x_i,t_n} + \frac{\Delta x^2}{2} \cdot \frac{\partial^2 u}{\partial x^2}|_{x_i,t_n} - \frac{\Delta x^3}{6} \cdot \frac{\partial^3 u}{\partial x^3}|_{x_i,t_n} + \frac{\Delta x^4}{24} \cdot \frac{\partial^4 u}{\partial x^4}|_{x_i,t_n} \tag{10}$$

By combining equations 8 and 10, and rearranging terms, one gets:

$$\frac{\partial^2 u}{\partial x^2}|_{x_i,t_n} = \frac{u_{i+1}^n - 2u_i^n + u_{i-1}^n}{(\Delta x)^2} + O\left[(\Delta x)^2\right] \tag{11}$$

By analogy, one can then also write:

$$\frac{\partial^2 u}{\partial t^2}\Big|_{x_i,t_n} = \frac{u_i^{n+1} - 2u_i^n + u_i^{n-1}}{(\Delta t)^2} + O\left[(\Delta t)^2\right] \tag{12}$$

Substituting (11) and (12) into the starting equation, 7, one finds:

$$u_i^{n+1} = (c\Delta t)^2 \cdot \frac{u_{i+1}^n - 2u_i^n + u_{i-1}^n}{(\Delta x)^2} + 2u_i^n - u_i^{n-1} + O\left[(\Delta t)^2\right] + O\left[(\Delta x)^2\right] \tag{13}$$

The so-called magic time step ($\Delta t = \Delta x/c$), which equates the temporal and spatial scales, one can find the spatio-temporal grid recursive relation:

$$u_i^{n+1} = (u_{i+1}^n - 2u_i^n + u_{i-1}^n) + 2u_i^n - u_i^{n-1} = u_{i+1}^n + u_{i-1}^n - u_i^{n-1} \tag{15}$$

For a plane wave traveling in the z-direction, the electric and magnetic field components follow scalar equation of the form eqn. 7:

$$\frac{\partial^2 \mathbf{E}_z}{\partial t^2} = c^2 \frac{\partial^2 \mathbf{E}_z}{\partial x^2} \qquad \frac{\partial^2 \mathbf{H}_y}{\partial t^2} = c^2 \frac{\partial^2 \mathbf{H}_y}{\partial x^2} \tag{16}$$

As such, both equations in (16) can be solved recursively by setting up a set of temporal and spatial grids. Of course, this approach can be generalized to four dimensions (three spatial and one temporal) in order to solve an arbitrary problem. Note also that any boundary conditions can also be accommodated in this method.

Generally speaking, the FDTD method is the more powerful one, since it has virtually no constraints. The drawback of this "brute-force" method is that the computational power necessary can become prohibitive. Nonetheless, we have to resort to this approach in order to determine the dynamical behavior, such as the lifetimes of the modes, which in turn determine the Q, for the three-dimensional confinement. Briefly, the EVP method would be first used to determine the mode structure. This mode will represent the initial condition in the FDTD code. The FDTD evolution will then run indefinitely, while keeping track of the field amplitude as a function of time. The resulting data will then be analyzed to determine (a) whether there is more than one time-

constant involved in the decay process, and (b) the dominant rate of decay. Of course, our goal would be to find the optimal parameters corresponding to the largest ratio of the vacuum Rabi frequency (proportional to the mean amplitude of the E field) and the cavity decay rate.

It is also obvious at this point that the FDTD method has to be used also for simulating the interaction between the quantized mode (i.e., photons) and the color centers, via the Jaynes-Cummings model, augmented by the Wigner-Weisskopf theory of spontaneous emission.

3.4 Adiabatic Evolution for Solving NP-Hard Optimization Problems

Fundamentally, a Quantum Computer is considered to be very powerful, with its computational ability growing exponentially with the number of coupled qubits. However, to this date, the type of problems that can be solved by a QC in a manner that is provably more efficient than classical computers has remained very limited. The most important example, of course, is the factoring algorithm, which can be performed by a QC (using Shore's algorithm) at a rate exponentially faster than conventional computers. The next important case is the Grover's algorithm, which enables a quadratic speed-up over classical methods. In parallel to these cases is the Type II quantum computing, which is expected to expedite the task of simulating complex processes such as turbulent flows to a rate far beyond the best classical super computers. Nonetheless, there is a class of problems for which it is yet to be shown that the QC computer can help. These are the so-called NP-Hard problems (NP: Non-deterministically Polynomial). Simply put, these are problems which are considered (but not proven; hence non-deterministic) to grow faster than any polynomial as a function of the size of the parameters. A classic example is the so-called traveling sales-man problem, where the sales-man would like to minimize the distance he has to travel in order to cover N-cities, where N is very large. It is generally observed that the difficulty of this minimization problem grows exponentially with N. This problem is also critical, for example, to the optimal scheduling of flights for commercial airlines. In general, there are a lot of optimization problems that fall under this category. As such, solving these class of problems efficiently is of great interest to the civilian sector as well as the DOD as a whole. In fact, this is considered the "holy-grail" of algorithm developments in computer science.

Given that QC and the NP-Hard problems both scale exponentially, it has long been expected that a QC would be solve this problem very efficiently (i.e., in a number of steps that is at most polynomial in the size of the problem, thus providing exponential speed-up over conventional methods). However, efforts by many groups have failed to find a QC algorithm for achieving this goal. Very recently, the group led by Farhi, in conjunction with several other groups, have developed a robust algorithm which appears to offer the solution. While it has not been proven rigorously, all evidence so far indicates that this approach --- termed Adiabatic Quantum Computation (AQC) --- is able to solve an NP-Hard problem in a number of steps that grows only polynomially with the size of the problem. We have developed a scheme for realizing AQC in the spin-based NV-Diamond quantum computing model that we are proposing to pursue

here. Before we describe our process, it is instructive to summarize briefly the notion of AQC.

The underlying notion is that an NP-Hard problem (or other problems, e.g., the Grover's search) can be modeled as the ground state of a number of interacting quantum bits. A specific example is the famous problem of the *Maximum Independent Set*: *Given a graph with V number of vertices and E number of edges, find the largest subset S of V such that no two vertices in S are joined by any edge E.* This problem is isomorphic to the two-dimensional Ising model, as illustrated in figure 1. Here, N spins are located at each of N vertices. The Hamiltonian for the Ising model is given by:

$$\hat{H}(t) = J(\sum_{vertices\ j} \hat{S}_j + \sum_{edges\ (i,j)} \hat{S}_i \hat{S}_j)$$

(17)

where, for all I, the spin operator S has the eigenvalues of 1 or -1, and the parameter J corresponds to the Zeeman splitting (i), which happens to be equal also to the antiferromagnetic coupling strength (i,j). Finding the solution to the problem of the maximum independent set is akin to finding the lowest energy eigenstate (LEE) of this Hamiltonian.

The process for finding the LEE can be formulated by writing the Hamiltonian in the following way:

$$\hat{H}(t)] = [1 - f(t)] \sum_{vertices\ j} \hat{\sigma}_Z^{(j)} + f(t)[\sum_{vertices\ i} \hat{\sigma}_x^{(i)} + \sum_{edges\ (i,j)} \hat{\sigma}_x^{(i)} \hat{\sigma}_x^{(j)}]$$

(18)

where f(t) monotonically increases from 0 (no coupling) to 1 (desired set of couplings), and σ represents the Pauli spinors. The f(t)=0 situation can be realized by cooling all the spins to their ground states, while the coupling is kept turned off. The coupling is then gradually turned on, reaching the f(t) =1. According to the adiabatic theorem of quantum mechanics, in order to ensure that the system evolves to the LEE, it is necessary that the inverse of the rate at which f(t) evolves from 0 to 1 is much less than the energy separation of the LEE of the couples system from the ground state of the uncoupled system. In all the cases studied so far[35-40], it has been found that this energy separation is typically large, allowing for a rapid switching-on of f(t), which in turn implies a QC based solution of the BP-Hard problem at a time scale that does not grow exponentially with the number of vertices. This approach of AQC has several key advantages over conventional quantum computing: (i) it does not require local qubit manipulation (e.g., no CNOT gates), and (ii) it is robust against noise, since there is no place to decay to from the ground state.

The NV-Diamond based Type-II QC we are proposing to build is ideally suited for this task. Briefly, the process will start by cooling all the spins to their uncoupled ground states. The coupling lasers will then be turned on slowly, and with the aid of the cavities, the system will evolve to the LLE of the interacting system. The coupling mechanism is exactly the same as what is described earlier in this proposal. Of course,

the scaling of the process will still limited by the total number of inter-coupled bits. Nonetheless, proving the feasibility of the AQC on a quantum computer, even with only 10's of qubits, will represent an important milestone in quantum information processing.

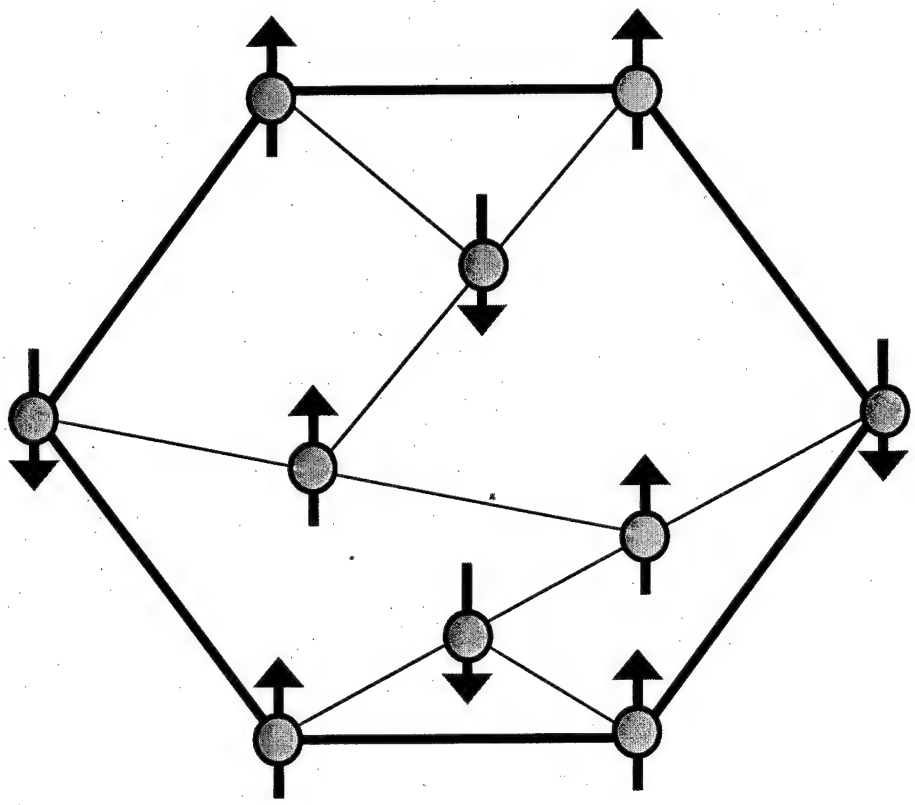

Figure 1: Schematic illustration of the two-dimensional Ising model, which is isomorphic to the problem of the Maximum Independent Set. See text for details.

3.5 Implementations of the Public Goods Game using Small-Scale Quantum Computers

In developing a Type-II QC, one is expected to build many small scale quantum computers (SSQC). One application of a set of SSQC we have identified is in the area of optimization of the Public Goods Game, which is an economic model representing a wide variety of social choice problems. For example, suppose that a group wishes to decide whether or not to provide a common good, such as a park, in the face of potential

free riders (i.e., those who will withhold payment but will nevertheless benefit from the common good). The free rider problem[1] cannot be solved in classical economics without either a third party to enforce agreements or a repeated game scenario in which participants can police themselves. Although government is one solution to this problem, it is an inefficient provider of public goods for smaller groups (such as a neighborhood watch). Invariably, contributions towards public goods at arbitrary scales are not made at efficient levels, and we seek a solution that (a) is efficient, (b) discourages free riders, and (c) avoids the need for a trusted third party. It has recently been shown that two-particle quantum entanglement can be used to solve this problem.[2]

The social dilemma is easy to understand using the following specific example of the economics of a public goods game that illustrates the core issues. Consider a game with N players, where player k starts the game with the private good x_k (e.g., his/her money). Each player then decides to contribute an amount c_k, so that the corresponding private good becomes $x_k' = x_k - c_k$. In the linear form of public good game, the resulting public good is MC, where $C = \sum_k c_k$ is the total contribution, and M is the production multiplier. This public good is then redistributed among the N players, so that player k's net gain (or "utility") is $u_k = MC/N - c_k$. Therefore, in the trivial cases where $M < 1$ and $M > N$, the efficient outcomes are clear: do not contribute, and contribute, respectively. However, in the more economically common case where $1 < M < N$, for any individual player $du_k / dc_k = M/N - 1 < 0$, and *it is rational for each player to choose not to contribute*, or to "free ride." In an economic context, this failure to encourage contribution to the public good is an inefficient outcome.

The quantum version of the public goods game (PGG) has three stages. In the first stage, an initial superposition state of a set of N identical quantum bits (qubits) is created and then entangled, with the resulting state made commonly known to all individuals. In the second stage, each player is allowed to choose an arbitrary quantum operator that acts on his or her individual qubit. In the last stage, the final superposition of the joint state is disentangled and then measured to produce a definite choice for each player.

The strategic space of the game is extended from the set of possible classical choices to the outer product of the set of all possible single-qubit unitary quantum operations on the state space. This approach is a direct quantum generalization of the original game, in that each player's operations should include actions that correspond to the classical choices: for each action in the classical game, there exists a quantum operation in the new game such that the outcome of the quantum game is the same as that of the original game, provided that all players are restricted to play the quantum operations that correspond to the classical choices. In other words, the quantum version of the game extends the strategic space from the set of possible classical actions to quantum operations acting on the set of possible classical actions.

Mathematically, the game proceeds as shown schematically in Fig. 1:

1. Starting with a particular initial superposition state $|\psi\rangle$ of N identical qubits, the entangled state $J|\psi\rangle$ is provided as a resource for the players, where J is an entanglement operator that commutes with the *classical* single-player operators.
2. Player k selects an operator U_k to apply to his or her entangled qubit, giving $|\psi'\rangle = (U_1 \otimes \cdots \otimes U_n) J|\psi\rangle$.

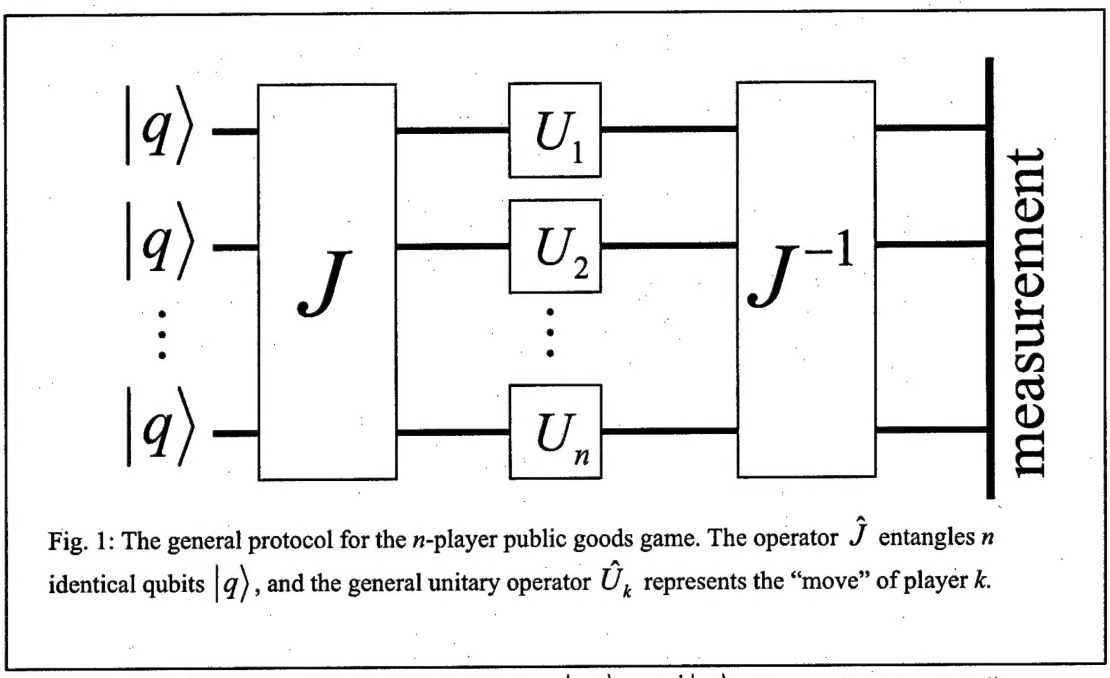

Fig. 1: The general protocol for the n-player public goods game. The operator $\hat{J}$ entangles n identical qubits $|q\rangle$, and the general unitary operator $\hat{U}_k$ represents the "move" of player k.

3. The qubits are "disentangled," giving $|\psi''\rangle = J^{-1}|\psi\rangle$. For a given game, (i.e., choices for $|\psi\rangle$ and J), the final superposition is a function of the players' choices of the particular operators $U_1, \ldots, U_n$.
4. The final state $|\psi''\rangle$ is measured, generating a specific value representing each player's choice. The probability of obtaining choice s (i.e., a particular assignment, 0 or 1, to each bit) is $|\langle s|\psi''\rangle|^2$.

The choice of J determines the type and degree of entanglement amongst the individual qubits of the players. The commutation condition on J ensures that if each player selects the operator corresponding to one of the choices in the classical game, the final result of the quantum game will, with probability 1, reproduce those choices.

Ideally, one would like the scheme to rely on the distribution of entangled states between distant players, implying that the qubits are encoded in the polarization states of photons transmitted throughout a fiber-optic network. Given a bright source of polarization-entangled photon pairs,[3] these qubits can be delivered by propagation through optical fibers, and purified using high-quality linear optical elements.[4] In principle, maximally entangled n-photon states can be constructed from entangled two-photon states,[5,6] and these states can be further manipulated using linear optical elements to perform universal gate operations.[7] In the context of Fig. 1, the initial state $|q\rangle\otimes|q\rangle\otimes\cdots\otimes|q\rangle$ and the entangling gate $\hat{J}$ can be constructed in one location, the players (who implement their strategies through the operators $\hat{U}_k$) can be geographically distributed over a wide area, and the disentangling gate and final measurement system can be placed in a third location.

However, scaling a fully entangled game from 2 to n players can be nontrivial even when linear optics is used. Suppose a trial between any two players succeeds with

probability β (incorporating the net efficiency with which entanglement can be created, distributed, purified, manipulated, and detected), so the mean number of trials needed to successfully register a mutual choice between two players is $1/\beta$. Because an accidental (or deliberately disruptive) measurement of a single qubit in the n-particle maximally entangled state destroys the entire state, we expect the number of trials needed to complete a maximally-entangled game for n players will scale no better than β^{-n}. Suppose instead we implement the game by distributing entangled two-particle states between either all enumerated pairs of players or nearest neighbors, as described previously. In these cases, we expect that the mean number of trials needed to complete the game will scale as either $n(n-1)/2\beta$ or n/β, and are therefore relatively easier to implement for games with a large number of players.

For example, in the simplest near-term implementation, a single game system can be constructed at a central location, and players can travel to the game and individually specify the operators to be applied to their qubits. As the technology evolves, the necessary hardware for specification of qubit operations can be distributed to distant players, who then can apply their operators to photonic qubits transported to them over an optical network. In either case, entangled pairs can be generated and distributed consecutively until all players have successfully registered a choice for each pair in which they are a member. Therefore, given some single-trial success probability β, the number of trials is limited by the rate at which two-particle entangled qubits can be provided. Although great strides continue to be made in multi-particle experiments,[5,6] it is clear that — until $\beta \to 1$ — two-particle games are far more feasible, and could allow tests of quantum game theory to be performed in the near future.

It has been shown that the n-player public goods problem can indeed be solved by exchanging entangled pairs of particles between n players using either of the topologies suggested above. The solutions are efficient, discourage free riders, and avoid the need for a trusted third party. However, because the game can be solved in this way by sequential exchanges of pairs, it is clear that it can be simulated classically and does not provide an exponential speed-up over classical mixed strategies. Instead, the significance of the quantum solution is similar to that of quantum key distribution: by using quantum mechanics, we replace an unverifiable trust mechanism (i.e., a third party) with a trust model based on the laws of quantum mechanics.

Let us examine the details of a two-player implementation of the public goods game, which is essentially equivalent to the Prisoner's Dilemma. We begin by choosing the Bell (EPR) basis $|\psi_{ij}\rangle$, $\{i,j\} \in \{0,1\}$, for our entangling and disentangling operators $\hat{J}$ and $\hat{J}^{-1}$, so that they can be constructed using Hadamard and CNOT gates as shown in Fig. 2. (In practice, the entangling gate $\hat{J}$ may be incorporated in the qubit source; as long as the entangled qubits are EPR pairs, the schematic of $\hat{J}^{-1}$ shown in Fig. 2 may be used.) The two players, Alice and Bob, play by specifying the unitary operators $\hat{U}_A$ and $\hat{U}_B$, respectively, each of which can be represented by the arbitrary unitary matrix

$$U(\alpha,\beta,\gamma) \equiv e^{-i\sigma_z\alpha/2} e^{-i\sigma_y\beta/2} e^{-i\sigma_z\gamma/2} = \begin{bmatrix} e^{-i(\alpha+\gamma)/2}\cos(\beta/2) & -e^{-i(\alpha-\gamma)/2}\sin(\beta/2) \\ e^{+i(\alpha-\gamma)/2}\sin(\beta/2) & e^{+i(\alpha+\gamma)/2}\cos(\beta/2) \end{bmatrix},$$

where σ_y and σ_z are two of the Pauli spin matrices. If we assume that the payoff for player k corresponding to the final state $|ij\rangle$ is p_{ij}^k, then the expectation value of the aggregate payoff for that player is $P^k = \sum_{\{i,j\}\in\{0,1\}} p_{ij}^k \left|\langle ij|\psi''\rangle^2\right|$.

Eisert et al.[8] have analyzed the quantum version of the Prisoner's dilemma, and have shown that the strategies given by $\hat{U}(0,\beta,0)$ are completely equivalent to classical mixtures of the identity and bit-flip operations, and offer no advantage over those classical strategies. Similarly, if "cooperation" is represented by the $|0\rangle$ state and defection by the $|1\rangle$ state, then the classical strategies "always cooperate" and "always defect" are represented by the operators $\hat{U}(0,0,0)$ and $\hat{U}(0,\pi,0)$, respectively. However, Eisert et al. also show that

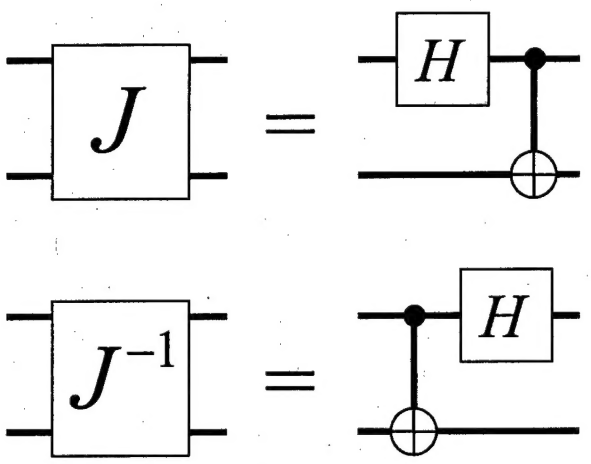

Fig. 2: A particular choice for the entangling and disentangling gates shown in Fig. 1. In this case, J creates the Bell basis states, and J^{-1} is the corresponding Bell state analyzer. Note that J^{-1} is the appropriate choice when the initial qubits are in fact created *ab initio* as entangled Bell states.

- if one player chooses the classical mixed strategy $\hat{U}(0,\beta,0)$, then the second player *always* wins using the strategy $\hat{U}(\pi,\pi/2,0)$; and
- there are a variety of quantum strategies available to each player that allow each to simultaneously achieve the optimum outcome.

In the context of the Prisoner's Dilemma, the optimum outcome — a new Nash equilibrium that is not available classically — allows the prisoners to rationally choose to cooperate and receive a relatively light sentence.

References

1. G. Hardin, Science 162, 1243 (1968).
2. K.-Y. Chen, T. Hogg, and R. Beausoleil, Quantum Information Processing 1, 449–469 (2002).
3. P. G. Kwiat et al., Phys. Rev. Lett. 83, 4725–4728 (1999).
4. J.-W. Pan, C. Simon, C. Brukner, and A. Zeilinger, Nature 410, 1067–1070 (2001).
5. D. Bouwmeester, J.-W. Pan, M. Daniell, H. Weinfurter, and A. Zeilinger, Phys. Rev. Lett. 82, 1345–1349 (1999).
6. J.-W. Pan, M. Daniell, S. Gasparoni, G. Weihs, and A. Zeilinger, Phys. Rev. Lett. 86, 4435– 4438 (2001).
7. E. Knill, R. Laflamme, and G. J. Milburn, Nature 409, 46–52 (2001).
8. J. Eisert, M. Wilkens and M. Lewenstein, Phys. Rev. Lett. 83, 3077–3088 (1999); Phys. Rev. Lett. 87, 069802 (2001).

4. TECHNOLOGY TRANSFER:

None.